Supplementary Information for

Nicotine Binding to Brain Receptors Requires a Strong Cation-π Interaction

Xinan Xiu, Nyssa L. Puskar, Jai A. P. Shanata, Henry A. Lester, and Dennis A. Dougherty*

*To whom correspondence should be addressed. E-mail: dadougherty@caltech.edu

Supplementary Figures

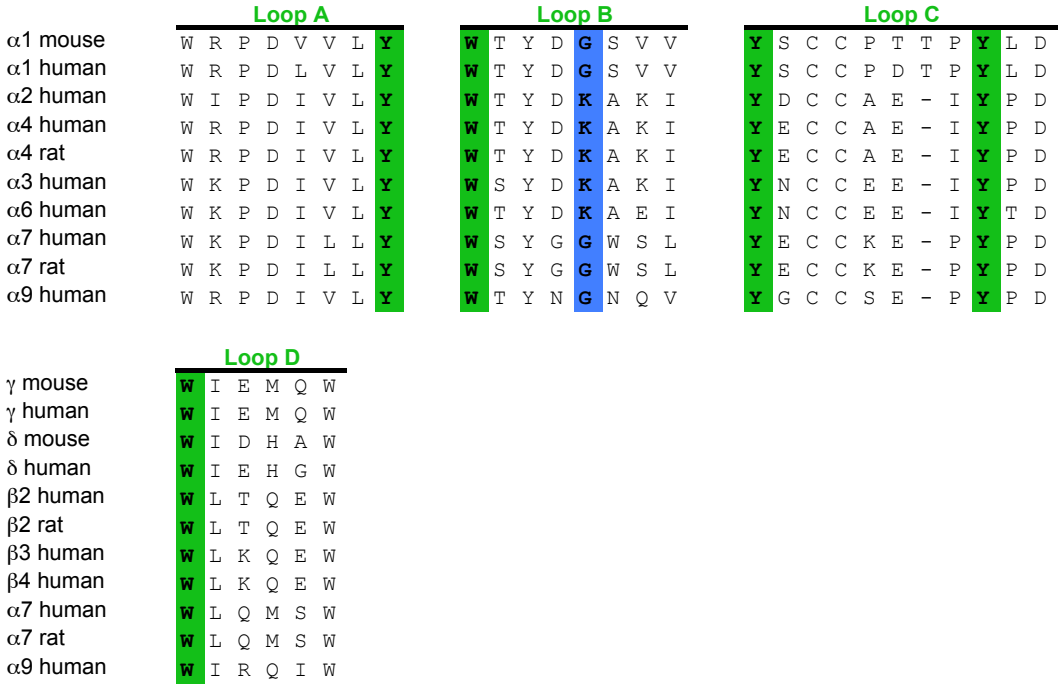

Supplementary Figure 1. Sequence alignment for Loops A, B, C, and D in the vicinity of the aromatic binding box. The five residues of the aromatic box: TyrA, TrpB, TryC1, TyrC2, and TrpD are highlighted in green. They are universally conserved in these subunits. G135 (α1) is the fourth residue after TrpB, highlighted in blue.

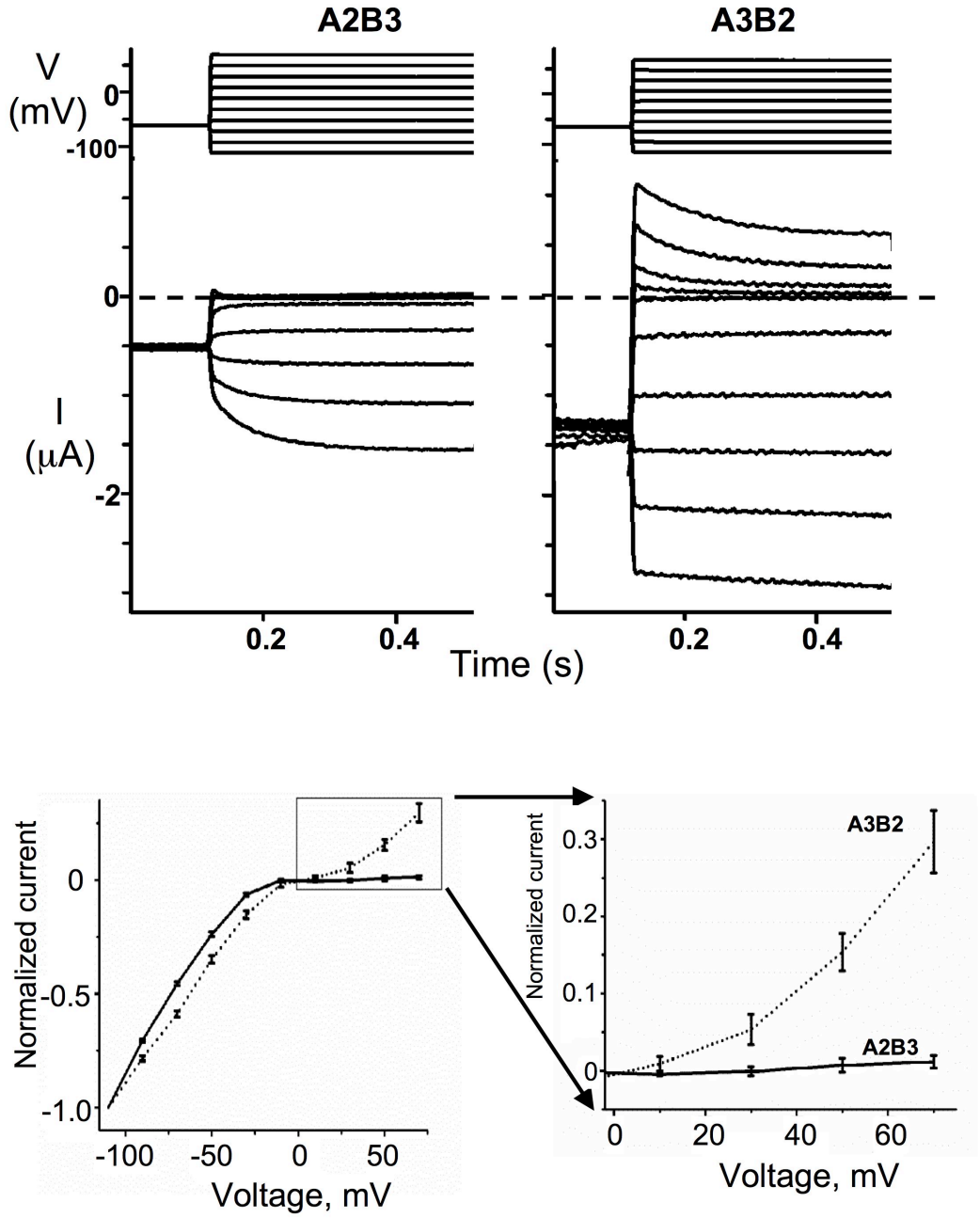

Supplementary Figure 2. Rectification behaviors of A2B3 and A3B2 L9'A α4β2 nAChR. Upper: Representative voltage traces and current responses for voltage jump experiments. Lower: I-V curves for A2B3 (solid line) and A3B2 (dotted line). The inset shows positive voltages, where A2B3 and A3B2 exhibit markedly different behavior.

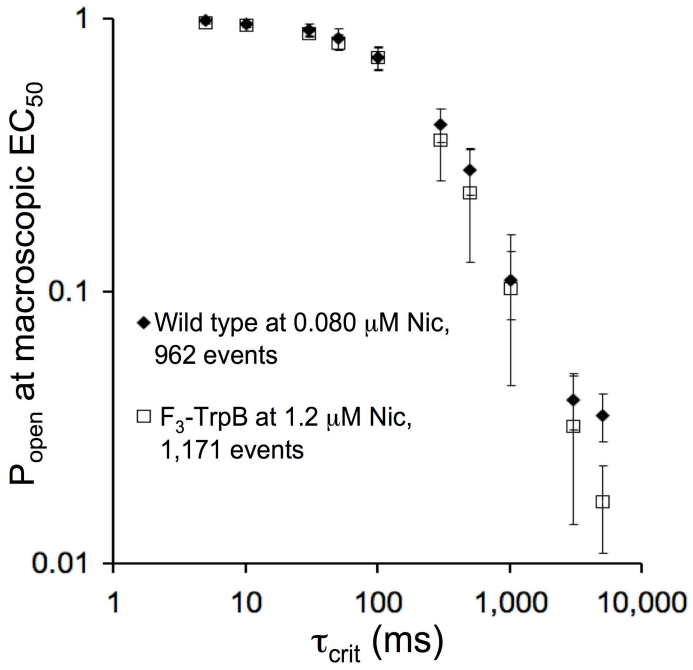

Supplementary Figure 3. Comparison of P_{open} at macroscopic EC_{50} for wild type and F_3-TrpB $\alpha4\beta2$ (A2B3) over a range of τ_{crit} values between 5 ms and 5000 ms reveals essentially equivalent gating behaviors. Error bars are mean ± s.e.m. and are smaller than the symbol when not shown.

Mutation	ACh	n_H	Nicotine	n_H	Norm. I (+70mV)
α4(L9'A)β2					
Wild type					
A2B3	0.42 ± 0.01	1.2 ± 0.1	0.08 ± 0.01	1.2 ± 0.1	0.041 ± 0.005
A3B2	0.023 ± 0.001	1.3 ± 0.1	0.01 ± 0.001	1.7 ± 0.2	0.297 ± 0.041
TyrA (Tyr98) A2B3					
Tyr	0.42 ± 0.03	1.2 ± 0.1	0.08 ± 0.01	1.7 ± 0.3	0.023 ± 0.009
Phe	12 ± 1	1.3 ± 0.1	0.77 ± 0.05	2.1 ± 0.3	0.064 ± 0.011
MeO-Phe	2.3 ± 0.2	1.2 ± 0.1	0.40 ± 0.02	1.7 ± 0.2	0.054 ± 0.032
F-Phe	15 ± 1	1.2 ± 0.1	0.32 ± 0.03	1.4 ± 0.2	-0.076 ± 0.046
F_2-Phe	16 ± 2	1.8 ± 0.3	0.39 ± 0.05	1.8 ± 0.4	0.028 ± 0.005
F_3-Phe	14 ± 1	1.2 ± 0.1	0.53 ± 0.04	1.4 ± 0.1	0.044 ± 0.010
Br-Phe	3.3 ± 0.2	1.2 ± 0.1	0.54 ± 0.04	1.5 ± 0.1	-0.003 ± 0.031
CN-Phe	73 ± 4	1.7 ± 0.1	8.8 ± 0.9	1.5 ± 0.2	0.075 ± 0.008
TrpB (Trp 154) A2B3					
Trp	0.44 ± 0.03	1.3 ± 0.1	0.09 ± 0.01	1.5 ± 0.1	0.006 ± 0.014
F-Trp	1.9 ± 0.1	1.2 ± 0.1	0.26 ± 0.02	1.3 ± 0.1	-0.065 ± 0.047
F_2-Trp	2.0 ± 0.1	1.3 ± 0.1	0.32 ± 0.04	1.3 ± 0.1	0.032 ± 0.025
F_3-Trp	13 ± 1	1.3 ± 0.1	1.2 ± 0.1	1.4 ± 0.2	-0.073 ± 0.029
F_4-Trp	29 ± 2	1.1 ± 0.1	4.2 ± 0.4	1.3 ± 0.2	-0.027 ± 0.023
CN-Trp	12 ± 1	1.2 ± 0.1	0.90 ± 0.07	1.4 ± 0.1	0.009 ± 0.017
Br-Trp	1.1 ± 0.1	1.3 ± 0.1	0.20 ± 0.02	1.3 ± 0.2	0.020 ± 0.005
TyrC1 (Tyr195) A2B3					
Tyr	0.42 ± 0.03	1.5 ± 0.1	0.07 ± 0.01	1.3 ± 0.1	0.042 ± 0.014
Phe	53 ± 4	1.3 ± 0.1	3.3 ± 0.2	1.2 ± 0.1	0.059 ± 0.014
MeO-Phe	48 ± 5	1.4 ± 0.2	2.8 ± 0.4	1.2 ± 0.2	0.064 ± 0.028
CN-Phe	210 ± 10	1.6 ± 0.1	19 ± 2	1.6 ± 0.2	0.057 ± 0.011
TyrC2 (Tyr202) A2B3					
Tyr	0.42 ± 0.03	1.3 ± 0.1	0.09 ± 0.01	1.6 ± 0.1	0.057 ± 0.016
Phe	0.32 ± 0.02	1.4 ± 0.1	0.14 ± 0.01	1.4 ± 0.1	0.014 ± 0.010
MeO-Phe	0.33 ± 0.02	1.3 ± 0.1	0.097 ± 0.006	1.7 ± 0.2	0.034 ± 0.033
CN-Phe	0.42 ± 0.04	1.4 ± 0.2	0.11 ± 0.01	1.6 ± 0.2	0.066 ± 0.046
Thr (B+1) (Thr 155) A2B3					
Thr	0.41 ± 0.02	1.4 ± 0.1	0.09 ± 0.01	1.6 ± 0.1	0.044 ± 0.007
Tah	0.37 ± 0.02	1.3 ± 0.1	1.71 ± 0.14	1.2 ± 0.1	0.018 ± 0.013
Muscle-type Receptor[a]					
Thr (B+1) (Thr150)[b]					
Thr	0.83 ± 0.04	1.8 ± 0.1	57 ± 2	2.1 ± 0.1	ND
Tah	0.25 ± 0.01	1.4 ± 0.1	92 ± 4	1.7 ± 0.1	ND

	α1(G153K)											
Trp	0.019	±	0.001	1.5	±	0.1	0.59	±	0.04	1.8	±	0.2	ND
F-Trp	0.094	±	0.004	1.6	±	0.1	2.8	±	0.1	1.3	±	0.1	ND
F_2-Trp	0.079	±	0.004	1.3	±	0.1	2.3	±	0.1	1.3	±	0.1	ND
F_3-Trp	1.05	±	0.03	1.3	±	0.1	11	±	1	1.5	±	0.1	ND
F_4-Trp	7.5	±	0.5	1.2	±	0.1	32	±	4	1.5	±	0.2	ND
CN-Trp	2.4	±	0.1	1.5	±	0.1	36	±	3	1.7	±	0.2	ND
Br-Trp	0.047	±	0.001	1.4	±	0.1	4.45	±	0.42	1.2	±	0.1	ND

Supplementary Table 1. EC_{50} values (μM), Hill coefficients (n_H) and current size at +70 mV (normalized to current size at -110 mV). ND = not determined. a. All studies of the muscle-type receptor contain a L9'S mutation in the β subunit. b. These values were previously reported[25].

Supplementary Discussion

Controlling the Stoichiometry of α4β2 Receptors

As in the case of previous studies, we find that the stoichiometry of α4β2 receptors can be controlled by altering the ratio of the subunits of mRNA during injection. Our criteria for defining a pure population of A2B3 α4(L9'A)β2 receptors are whole-cell dose-response curves that fit a single component and very strong inward rectification such that (I_{max} at +70 mV)/(I_{max} at -110 mV) < 0.1. An alternative analysis which can also demonstrate a mixed population of receptors is the production of intermediate EC_{50} values when fit to a single component. As shown below, by a 3:1 α4:β2 mRNA ratio, the EC_{50} value has reached the higher EC_{50} value, which is the A2B3 stoichiometry.

α4:β2 ratio	EC_{50} (μM ACh)
100:1	0.023 ± 0.002
10:1	0.023 ± 0.001
6:1	0.15 ± 0.02
3:1	0.44 ± 0.03
1:1	0.40 ± 0.01
1:10	0.43 ± 0.02

Injection of an mRNA ratio α4(L9'A):β2 of 10:1 or higher produces pure populations of A3B2, while a ratio of 1:3 or lower guarantees a pure population of A2B3. In the experiments described here, we injected a 1:3 ratio of mRNA.

Note that the α4(L9′A) mutation lowers EC_{50} in a multiplicative fashion, depending on how many α4 subunits are present. As such, our A3B2 receptor (with three L9′A mutations) actually has a lower EC_{50} than our A2B3 receptor (with two L9′A mutations), even though the binding site from the A2B3 stoichiometry is clearly that of the high sensitivity receptor.

TyrA, TyrC1, and TyrC2 Display Similar Interactions in Muscle-type and α4β2

In addition to TrpB, we have performed extensive studies of other aromatic residues in and around the aromatic box (Supplementary Table 1). Briefly, when comparing α4β2 to the muscle-type receptor, very similar results are seen. TyrC1 is very sensitive to substitution, establishing a key role for this residue, likely in receptor gating. TyrA appears to be a hydrogen

bond donor (large effects for Phe and MeO-Phe substitutions), and while it is generally more sensitive to perturbations in the neuronal receptor, the basic trends are the same. TyrC2 is very permissive in both the muscle-type and $\alpha4\beta2$ receptors.

Single-Channel Recording and Analysis

Here we have used single-channel measurements to convincingly establish that the fluorination approach is changing agonist binding, not channel gating. Macroscopic data establish the large successive shift in function (EC_{50}) upon fluorination, and single-channel data establish that gating is unperturbed, since the probability that the channel is open, P_{open}, is essentially indistinguishable for wild type and F_3-TrpB at corresponding points on the dose-response relation. At saturating agonist concentrations, $P_{open,max}$ approaches $\Theta/(\Theta+1)$. Our analysis starts by comparing the P_{open} values at the macroscopic EC_{50}. The P_{open} values that we report are directly related to the gating equilibrium constant, Θ, by $\frac{1}{2} * \Theta/(\Theta+1)$.

Definition of clusters and calculation of P_{open}

Because (a) single-channel channel measurements of P_{open} are seldom reported for $\alpha4\beta2$ receptors, and (b) we find that P_{open} depends strongly on the value chosen as the critical closed duration, τ_{crit}, we report P_{open} values for the range 5 ms $\leq \tau_{crit} \leq$ 5000 ms using two different methods to identify τ_{crit} (below and Supplementary Fig. 3, above). The first is the commonly used method: the longest one or more components of the closed dwell time histogram are considered as sojourns in the desensitized state for all of the channels in the patch[32]. The value for τ_{crit} was defined based on the closed dwell time histograms fitted with multiple components, as previously described[33]. These components are similar for wild type and F_3-TrpB, resulting in similar τ_{crit} values: τ_{crit1} of 1470 vs 1530 ms and τ_{crit2} of 42 vs 52 ms, respectively. The similarity of the closed dwell time histograms for these receptors (and the resultant τ_{crit} values) can be taken as evidence that fluorination does not significantly impact desensitization. Moreover, whole-cell data show that the wild type and the F_3-TrpB receptors exhibit similar extent and kinetics of macroscopic desensitization (data not shown). When either of the τ_{crit} values calculated from the closed dwell time histogram is applied, P_{open} is essentially indistinguishable

for wild type and F_3-TrpB. The P_{open} values for wild type and F_3-TrpB at τ_{crit1} and τ_{crit2} are given here ± s.e.m.

Receptor	P_{open} (τ_{crit1})	P_{open} (τ_{crit2})
Wild type	0.07 ± 0.02	0.88 ± 0.06
F_3-TrpB	0.06 ± 0.03	0.82 ± 0.05

Because our recordings are at an intermediate concentration (EC_{50}), some closed dwells may reflect agonist dissociation, others may reflect channel closure followed by re-opening without agonist dissociation, while still others may reflect sojourns in desensitized states of varying duration. As a result, a definition of τ_{crit} can be distorted by the relatively low number of long non-conducting sojourns. Thus, we also compared calculated P_{open} values for a wide range of possible τ_{crit} values (3 orders of magnitude), including those calculated from the closed dwell time histogram. Supplementary Fig. 3 shows that, regardless of how we define τ_{crit} (5 ms $\leq \tau_{crit} \leq$ 5000 ms), no systematic difference in P_{open} is observed between wild type and F_3-TrpB with nicotine as agonist—their gating behaviors are essentially indistinguishable. Thus, the value chosen for τ_{crit} does not affect our conclusion that the gating behavior, as measured by P_{open}, is not significantly impacted upon fluorination in the F_3-TrpB mutant.

A small shift in the channel open duration does not account for the EC_{50} shift of F_3-TrpB

Fits to open dwell time histograms reveal that the main component of the channel open duration, which accounted for >90% of the conductance in both wild type and F_3-TrpB receptors, is shifted 2.4-fold, from 23 ms (wild type) to 9.6 ms (F_3-TrpB). Because the closed dwell time histograms, fitted with multiple components, displayed similar contributions from the major components for wild type and F_3-TrpB, interpreting the 2.4-fold shift in open duration in terms of the channel closing rate, α, would imply a modest 2.4-fold shift in Θ in the F_3-TrpB receptor. We consider these results in terms of a standard, linear 4-state model with two sequential agonist binding steps followed by a gating step:

$$A + R^c \underset{k_{-1}}{\overset{2k_1}{\rightleftharpoons}} A + AR^c \underset{2k_{-1}}{\overset{k_1}{\rightleftharpoons}} A_2R^c \underset{\alpha}{\overset{\beta}{\rightleftharpoons}} A_2R^o$$

for which,

$$EC_{50} = \frac{K_D}{\sqrt{\Theta + 2} - 1}$$

where K_D is the equilibrium agonist dissociation constant (k_{-1}/k_1) and Θ is the gating equilibrium constant (β/α). We see that a 2.4-fold change in Θ accounts for at most a 1.5-fold shift in EC_{50}. Thus, both comparison of P_{open} as well as consideration of kinetics, to the extent possible for data at EC_{50}, indicate that the overwhelming majority of the 15-fold increase in nicotine's EC_{50} in the F_3-TrpB receptor versus wild type is caused by changes to binding rather than the subsequent conformational changes that open the channel. Taken together, macroscopic and single-channel experiments show that fluorination modulates nicotine binding in a way that is systematically correlated to the energy of a cation-π interaction.

Supplementary Notes

[32] Sakmann, B., Patlak, J., and Neher, E., Single acetylcholine-activated channels show burst-kinetics in presence of desensitizing concentrations of agonist. *Nature* **286** (5768), 71 (1980).

[33] Jackson, M. B. et al., Successive openings of the same acetylcholine receptor channel are correlated in open time. *Biophysical journal* **42** (1), 109 (1983).